THE JOURNAL OF BIOLOGICAL CHEMISTRY VOL. 285, NO. 20, pp. 14909–14919, May 14, 2010

Role of Protein Misfolding in DFNA9 Hearing Loss*[S]

Received for publication, January 25, 2010, and in revised form, March 11, 2010 Published, JBC Papers in Press, March 12, 2010, DOI 10.1074/jbc.M110.106724

Jianhua Yao[‡], Bénédicte F. Py[‡], Hong Zhu[‡], Jianxin Bao[§], and Junying Yuan[‡1]

From the [‡]Department of Cell Biology, Harvard Medical School, Boston, Massachusetts 02115 and the [§]Department of Otolaryngology, Washington University, St. Louis, Missouri 63110

Mutations in the *COCH* (coagulation factor C homology) gene have been attributed to DFNA9 (deafness, autosomal-dominant 9), an autosomal-dominant non-syndromic hearing loss disorder. However, the mechanisms responsible for DFNA9 hearing loss remain unknown. Here, we demonstrate that mutant cochlin, the protein product of the *COCH* gene, forms a stable dimer that is sensitive to reducing agent. In contrast, wild-type (WT) cochlin may form only dimers transiently. Interestingly, the presence of mutant cochlin can stabilize WT cochlin in dimer conformation, providing a possible mechanism for the dominant nature of DFNA9 mutations. Furthermore, the expression of mutant cochlin eventually induces WT cochlin to form stable oligomers that are resistant to reducing agent. Finally, we show that mutant cochlin is cytotoxic *in vitro* and *in vivo*. Our study suggests a possible molecular mechanism underlying DFNA9 hearing loss and provides an *in vitro* model that may be used to explore protein-misfolding diseases in general.

Protein misfolding is a fundamental mechanism underlying multiple chronic neurodegenerative diseases, including Alzheimer disease, Huntington disease, and prion disease, which have been called collectively the conformational diseases to emphasize the role of aberrant protein conformations in the clinical manifestation of the diseases (1). Mutations of different genes involved in these diseases have been shown to lead to oligomerization and aggregation of corresponding proteins to form amyloid. The conformational transition that leads to the formation of amyloid requires misfolding of native protein structure and intermolecular bonding. However, we still understand very little about the conformational transition processes from the misfolded state to the aggregated state, as this transition for most conformational disease-associated mutant proteins explored so far is both rapid and heterogeneous.

Point mutations in the *COCH* (coagulation factor C homology) gene are responsible for an autosomal-dominant non-syndromic hearing disorder termed DFNA9 (deafness, autosomal-dominant 9) (2). DFNA9 is characterized by adult-onset, progressive neurosensory hearing loss with vestibular dysfunction. Pathological studies of the temporal bones from affected individuals have shown remarkable degeneration of neuroepithelial cells, including both fibrocytes and neurosensory cells, and the accumulation of abundant acellular eosinophilic deposits throughout the auditory and vestibular systems (3, 4). However, the mechanism responsible for the degeneration and hearing loss in DFNA9 syndrome remains unknown.

The amino acid sequence of cochlin, the protein product of the gene *COCH*, is highly conserved in mammals (5). The deduced amino acid sequence of cochlin contains a signal peptide in its N terminus, followed by a region homologous to a domain in the FCL domain (factor C of *Limulus*; also named the LCCL domain for *Limulus* factor C/Coch-5b2/Lgl1), a short intervening domain, and two von Willebrand factor A-like domains separated by a second short intervening domain. The von Willebrand factor A-like domain is known to function by interacting with extracellular matrix proteins such as collagen (6). The LCCL domain is a novel fold consisting of a central α-helix wrapped on two sides by irregular secondary structures that include eight short β-strands stabilized by two pairs of disulfide bonds (7). Because most of the disease-associated point mutations in *COCH* are localized in the LCCL domain of cochlin (8), the function of the LCCL domain is predicted to play a critical role in the pathogenesis of DFNA9. *Coch*$^{-/-}$ mice do not develop the degeneration and hearing loss as observed in DFNA9 patients, suggesting that DFNA9-associated *COCH* mutations may be gain of function in nature (9). It is not clear, however, how disease-associated mutations in *COCH* convey a toxic gain of function.

The normal function of cochlin is also unknown. The expression of COCH is highly enriched in the inner ear but can also be detected in other organs (2, 10). Five isoforms (p63, p44, p40, p18, and p16) of cochlin were found in adult bovine cochlea (11, 12), and two isoforms were found in fetal human inner ear (p60 and p50) (13). Cochlin comprises the major non-collagen component of the extracellular matrix predominantly present in the spiral ligament and spiral limbus regions in fetal and adult mouse and human inner ears, corresponding to the regions of abnormalities in DFNA9 (13).

The abundant acellular eosinophilic deposits throughout the cochlear and vestibular systems of DFNA9 patients (3) and the tendency of the recombinant mutant LCCL domains to misfold *in vitro* (7) have led to the proposal for a potential involvement of protein misfolding in DFNA9. However, no direct evidence for misfolding of mutant cochlins has been demonstrated. In cultured cells, wild-type (WT)[2] and mutant cochlins are synthesized, modified, and secreted in similar amounts (14, 15). Thus, mutant cochlins are able to be glycosylated and secreted

* This work was supported, in whole or in part, by the National Institutes of Health Director's Pioneer Award (to J. Y.).

[S] The on-line version of this article (available at http://www.jbc.org) contains supplemental Figs. 1 and 2.

[1] To whom correspondence should be addressed. Tel.: 617-432-4170; Fax: 617-432-4177; E-mail: junying_yuan@hms.harvard.edu.

[2] The abbreviations used are: WT, wild-type; CM, conditioned medium; HA, hemagglutinin; ABR, auditory brainstem response; CTF, C-terminal fragment; NTF, N-terminal fragment.

adequately by cells through the Golgi/endoplasmic reticulum secretory pathway. The cellular behavior of mutant cochlins is different from that of other known intracellular and extracellular misfolded mutant proteins such as mutant Htt (16) and β-amyloid (17), which readily form high order oligomers upon expression. These results have led to the suggestion that DFNA9 mutations may manifest deleterious effects beyond the point of secretion in the extracellular matrix of the inner ear by disrupting cochlin function or interfering with protein-protein interactions involving the LCCL domain. However, although WT cochlin accumulates in extracellular deposits that closely parallel the matrix component fibronectin, no consistent deposition of mutant cochlin was found (14).

In this study, we show that although mutations in the *COCH* gene do not consistently affect the secretion of cochlin, they lead to dimerization and oligomerization of intracellular and secreted cochlins. Interestingly, the presence of mutant cochlin is able to induce WT cochlin to form reducing agent-sensitive dimers and eventually reducing agent-insensitive oligomers. We further reveal that the coexpression of mutant and WT cochlins is cytotoxic for cells of inner ear origin *in vitro* and *in vivo*. Our study demonstrates the interaction of WT and mutant proteins, the role of WT protein in protein-misfolding diseases, and a potential molecular mechanism for co-dominance of WT and mutant proteins in mediating selective degeneration in age-delayed chronic neurodegenerative diseases.

EXPERIMENTAL PROCEDURES

Generation of Mammalian Expression Constructs—Full-length mouse *Coch* cDNA was amplified by PCR from a mouse spleen library (18) and subcloned into the pcDNA3.1(+) vector (Invitrogen) and the pFLAG-CMV5 (Sigma) and pMH (Roche Applied Science) vectors, respectively. Point mutations were introduced using the QuikChange site-directed mutagenesis kit (Stratagene, La Jolla, CA) according to the manufacturer's protocol. Anti-active caspase-3 antibody was from Cell Signaling (Beverly, MA).

Cell Culture and Transfection—UB/UE-1 cells, kindly provided by Dr. Mathew Holley (19), were maintained at 33 °C in complete medium plus 50 units/ml recombinant murine interferon-γ (R&D Systems, Inc., Minneapolis, MN). UB/UE-1 cells were induced to differentiate by culturing at 39 °C in complete medium without recombinant murine interferon-γ. Primary fibrocytes were isolated from mouse cochlea following a previously described protocol (20).

293T cells were allowed to grow to 70~80% confluence and transfected with constructs with TransIT polyamine transfection reagents (Mirus Corp., Madison, WI). UB/UE-1 cells were transfected with the Amaxa Nucleofector and Cell Line Nucleofector Kit R, Program T-27 (Amaxa Inc.). The conditioned medium (CM) of 293T cells collected for intracochlear injection did not contain 10% fetal bovine serum, 1% penicillin/streptomycin, or phenol red. CM was concentrated ~8-fold by centrifugal filter units with microporous membrane. HeLa cells were grown in Dulbecco's modified Eagle's medium + 10% fetal calf serum and transfected with TransIT reagent.

Immunoblotting and Immunoprecipitation Analysis—Forty-eight hours after transfection, 293T cell culture supernatant was collected. Cells were then washed once with cold phosphate-buffered saline and solubilized in radioimmune precipitation assay buffer (150 mM NaCl, 1% Nonidet P-40, 0.5% sodium deoxycholate, 0.1% SDS, and 50 mM Tris, pH 8.0) supplemented with Complete protease inhibitor mixture (Roche Applied Science). After incubation at 4 °C for 30 min, samples were centrifuged at 16,000 ×*g* for 30 min, and culture supernatants were collected. The samples were mixed at a 1:1 ratio either with nonreducing loading buffer (50 mM Tris, pH 6.8, 10% glycerol, 2% SDS, and 0.5% bromphenol blue) and not heated for nonreducing SDS-PAGE or with reducing loading buffer (50 mM Tris, pH 6.8, 10% glycerol, 2% SDS, 5% β-mercaptoethanol, and 0.5% bromphenol blue) and heated at 95 °C for 10 min for reducing SDS-PAGE. Cell lysates were separated either by nonreducing SDS-PAGE in the absence of β-mercaptoethanol or by reducing SDS-PAGE in the presence of β-mercaptoethanol.

Immunoprecipitation was accomplished using agarose beads conjugated with anti-FLAG monoclonal antibody M2 (Sigma) or with anti-hemagglutinin (HA) monoclonal antibody (Santa Cruz Biotechnology) for 2 h at 4 °C with rotation from supernatants or cell lysates collected from 5×10^6 293T cells expressing vector only or cochlins. After the beads were washed four times with radioimmune precipitation assay buffer, FLAG-tagged cochlins were eluted in 100 μl of radioimmune precipitation assay buffer containing 250 mg/ml FLAG peptide (Sigma) for 1 h at 4 °C or by heating (for HA).

Cell Death Analysis—UB/UE-1 cells were transfected by the Nucleofector system. The cells were maintained either at 33 °C (undifferentiated) or at 39 °C (differentiated). Seventy-two hours after transfection, dead and living cells containing green fluorescent protein were counted visually.

Intracochlear Injection and Hearing Test—C57BL/6 mice (4~6 weeks old) were chosen as the recipients. The surgical procedure was performed, and 10 μl of CM containing either WT or mutant cochlin was injected from the lateral semicircular canal using the procedure described previously (21, 22). The hearing threshold for each animal was measured by auditory brainstem response (ABR) testing 1 and 4 weeks after the protein injection as described (23).

Tissue Preparation and Histology—Mice were anesthetized with a mixture of ketamine (80 mg/kg) and xylazine (16 mg/kg) given intraperitoneally, and mouse cochleae were processed as described (24) and stained with Mayer's hematoxylin solution.

Immunofluorescence Microscopy—HeLa cells were fixed with 4% paraformaldehyde, treated with 0.1 M glycine, and permeabilized in 0.1% Triton X-100 + 0.2% bovine serum albumin. Cells were then subsequently stained with anti-FLAG antibody M2, Alexa 488-conjugated anti-mouse IgG antibody (Molecular Probes), mouse serum (1:100), and Alexa 594-conjugated anti-HA antibody (Molecular Probes). Cells were imaged on a Nikon TE2000E inverted fluorescence microscope as Z-series (0.25 μm) using a 60× objective lens. *Z*-stacks were deconvolved using AutoQuant X2 software (AutoQuant Imaging, Inc.), followed by three-dimensional reconstruction using MetaMorph software (Molecular Devices).

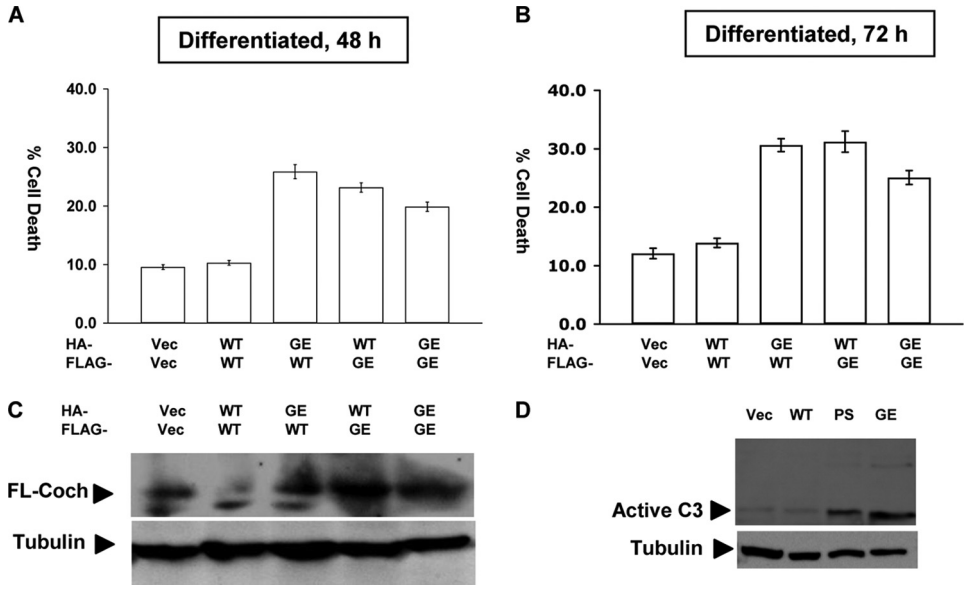

FIGURE 1. **Cell death induced by coexpressing WT and mutant cochlins.** UB/UE-1 cells were cotransfected with HA- and FLAG-tagged WT and mutant G90E (*GE*) cochlins as indicated. Cell death was measured after UB/UE-1 cells were transfected for 48 h (*A*) or 72 h (*B*) by counting green fluorescent protein-positive live *versus* dead cells. At least 200 cells were counted for each of treatment, and at least three independent experiments were performed. Total cochlin expression was determined by Western blotting using anti-LCCL monoclonal antibody against cochlin (*C*). Activation of caspase-3 was detected by Western blotting using anti-active caspase-3 antibody (*D*). Student's *t* test was applied for statistical analysis. *Vec*, vector; *FL-Coch*, full-length cochlin; *PS*, P53S.

RESULTS

Expression of Mutant Cochlin Induces Cell Death of Inner Ear Origin—Because degenerative hearing loss is a hallmark of DFNA9, we hypothesized that mutant cochlin may function as a proteotoxic species that leads to cell death. To test this hypothesis, we utilized UB/UE-1 cells, a cell line derived from progenitor cells of the mouse inner ear. Cochlin is expressed abundantly in the inner ear and has been reported to represent as much as 70% of the extractable proteins in the bovine inner ear (11). On the other hand, the expression of cochlin in UB/UE-1 cells is much lower than that *in vivo* (data not shown). To create a condition comparable with the expression of cochlin *in vivo*, we transfected the expression vectors of murine WT and mutant G90E cochlins, corresponding to the DFNA9-associated G88E mutation in humans, into UB/UE-1 cells. Interestingly, expression of mutant cochlin or WT and mutant cochlins together but not WT cochlin alone in differentiated UB/UE-1 cells induced cell death associated with activation of caspase-3 (Fig. 1, *A–D*). In contrast, expression of WT and/or mutant cochlin in 293T or HeLa cells was not cytotoxic (data not shown). Thus, expression of mutant cochlin leads to cytotoxicity in cells derived from the inner ear.

Secretion and Processing of Wild-type and Mutant Cochlins—Cochlin was predicted to be a secreted protein based on its N-terminal signal peptide and von Willebrand factor A-like domains, which are usually found in proteins associated with the extracellular matrix (25). We developed two specific anti-cochlin antibodies, an anti-LCCL monoclonal antibody and an anti-C-terminal fragment (CTF) polyclonal antibody. The anti-LCCL antibody recognizes the LCCL domain, whereas the anti-CTF antibody recognizes the N-terminal part of the C-terminal domain (CTF) of cochlin as well as the LCCL domain (supplemental Fig. 1). Because the cochlin isoforms expressed from the expression vector of full-length *COCH* cDNA, including full-length cochlin, CTF, N-terminal fragment (NTF) A, and NTF-B, migrated similarly on SDS-polyacrylamide gel as the endogenous cochlin isoforms in the inner ear cell lysate (supplemental Fig. 1), we conclude that our culture model recapitulates key behaviors of endogenous cochlin in processing and secretion.

Using this system, we explored the processing of WT and mutant cochlins in HEK293T cells transiently transfected with expression vectors of WT and mutant cochlins. We followed the maturation of WT cochlin by Western blotting using anti-LCCL and anti-CTF antibodies. On Western blots, anti-CTF antibody recognized secreted WT cochlin predominantly as the CTF (44 kDa) as well as a small amount of full-length cochlin (Fig. 2*A*). At later time points, two additional cochlin species, NTF-A (18 kDa) and later NTF-B (16 kDa), both derived from the LCCL domain, were detected in the culture supernatant. On Western blots of the supernatant using anti-LCCL antibody, which recognizes the LCCL domain only, we first detected full-length cochlin, followed by NTF-A and then NTF-B (Fig. 2*B*). Interestingly, the amount of secreted full-length cochlin (63 kDa) in the culture supernatant remained constant over 24 h, whereas the amount of the smaller fragments of other cochlin species (CTF, NTF-A, and NTF-B) increased over time. Importantly, the processing of WT cochlin as detected by both antibodies is entirely consistent. The kinetic difference in the detection of full-length *versus* mature cochlin isoforms in the culture supernatant suggests that the smaller isoforms, especially NTF-A and NTF-B, are produced by the cleavage of full-length cochlin at the cell surface.

We also analyzed the secretion of cochlin mutants associated with DFNA9 syndrome. Because the amino acid sequences of murine and human cochlins are 94% identical, we introduced four point mutations, P53S, V68G, G90E, and W119R, into murine WT cochlin, corresponding to the human DFNA9 mutations of P51S, V66G, G88E, and W117R, respectively. The expression vectors of WT and mutant cochlins were transfected into 293T cells, and the culture supernatants were analyzed by Western blotting using anti-CTF (Fig. 2*C*) and anti-LCCL (Fig. 2*D*) antibodies. Compared with WT cochlin, all mutants analyzed showed a varying degree of increases in the levels of full-length cochlin and decreases in the levels of processed forms (CTF, NTF-A, and NTF-B). In the culture supernatant of 293T cells expressing P53S and W119R, there was a slight increase in the full-length cochlin/CTF ratio compared

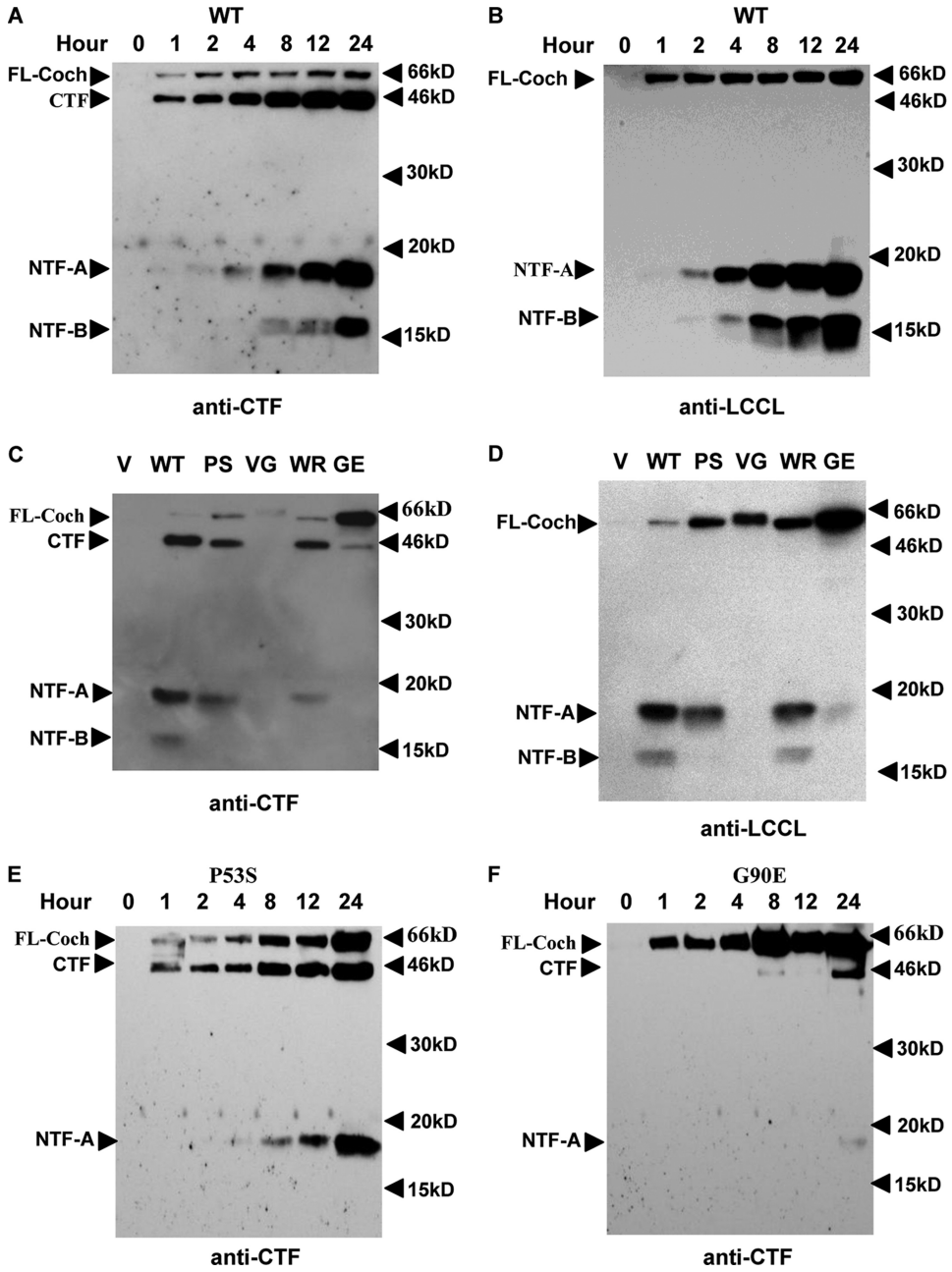

FIGURE 2. **Dynamics of cochlin secretion.** WT (*A* and *B*) and mutant (*C–F*) cochlin expression vectors were transiently transfected into HEK293T cells, and the culture supernatant was collected at the indicated time points (*A*, *B*, *E*, and *F*) and analyzed by Western blotting using anti-CTF polyclonal antibody (*A*, *C*, *E*, and *F*) or anti-LCCL monoclonal antibody (*B* and *D*) after separation by 15% reducing SDS-PAGE. The results shown are representative of three separate experiments. *FL-Coch*, full-length cochlin; *V*, vector; *PS*, P53S; *VG*, V68G; *WR*, W119R; *GE*, G90E.

with WT cochlin (Fig. 2*C*). On the other hand, the increase in the full-length cochlin/CTF ratio was much more dramatic in the culture supernatant expressing V68G and G90E, which showed very little detectable CTF (Fig. 2, *C* and *D*). This conclusion is also supported by a time course study of mutants P53S and G90E (Fig. 2, *E* and *F*). Although the production of CTF and NTF-A for P53S cochlin is largely normal, the processing of G90E cochlin is highly defective. In addition, these mutations also affected the processing of the N-terminal LCCL domain isoforms, namely NTF-A and NTF-B. On Western blots probed with anti-CTF antibody, there was a severe reduction of both NTF-A and NTF-B in the supernatant expressing all the point mutants. On the other hand, because the anti-LCCL antibody is much more sensitive in detecting the LCCL domain compared with the anti-CTF antibody (supplemental Fig. 1), the anti-LCCL antibody detected variable amounts of NTF-A and NTF-B on the same Western blot of the culture supernatant expressing different mutants, with the exception of W119R, which expressed approximately the same amount of NTF-A and NTF-B as WT cochlin (Fig. 2*D*). The variable effects of different mutations on the processing of secreted mutant cochlins were further confirmed by a time course study of the P53S and G90E mutants (Fig. 2, *E* and *F*). Because the V68G mutation almost completely abolished the production of CTF, NTF-A, and NTF-B, whereas the W119R mutation appeared to have a minimal effect, we conclude that DFNA9-associated *COCH* mutations have variable effects on the processing and/or secretion of cochlin and that at least some of the mutants are processed and secreted normally similar to WT cochlin. Consistent with this proposal, we found that the subcellular distributions of WT and mutant cochlins are very similar (supplemental Fig. 2), which is consistent with what was reported by Robertson *et al.* (15).

Excessive Dimerization of Cochlin Mutants—To understand how mutant cochlin causes cytotoxicity, we investigated the effects of the mutations on protein folding. We developed an assay using nonreducing SDS-PAGE in the absence of β-mercaptoethanol in conjunction with Western blotting. The WT and mutant cochlin expression constructs were transfected into HEK293T cells individually, and the culture supernatant and cell lysate were collected under nonreducing conditions for Western blotting using anti-CTF polyclonal antibody (Fig. 3, *A* and *E*) and anti-LCCL monoclonal antibody (Fig. 3, *B* and *F*) after SDS-PAGE in the absence of reducing agent. The full-length WT and CTF cochlins in the culture supernatant and cell lysates, which ran as 63- and 44-kDa bands upon reducing SDS-PAGE, respectively (Fig. 2*C*), migrated also as 63- and 44-kDa bands upon nonreducing SDS-PAGE (Fig. 3, *A* and *E*). Thus, the migratory behavior of WT

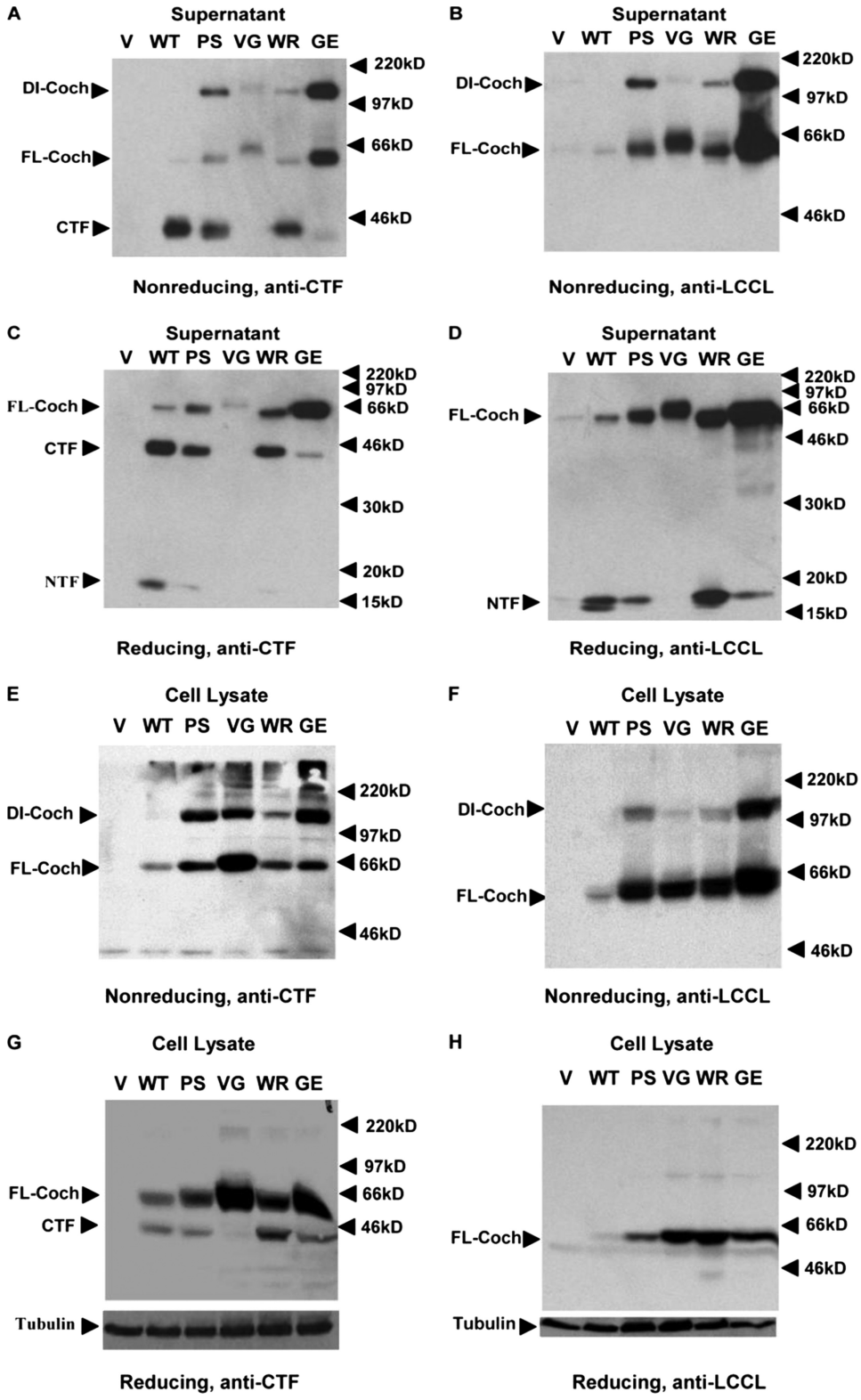

FIGURE 3. ***COCH* mutations induce the formation of a 120-kDa mutant complex intracellularly and extracellularly.** The culture supernatant (*A–D*) or cell lysates (*E–H*) from transiently transfected HEK293T cells expressing the control vector (*V*), the WT *COCH* gene, or mutant P53S (*PS*), V68G (*VG*), G90E (*GE*), or W119R (*WR*) *COCH* were separated by 8% nonreducing SDS-PAGE (*A*, *B*, *E*, and *F*) or by 12% (*C* and *D*) or 10% (*G* and *H*) reducing SDS-PAGE. The Western blots were probed with anti-CTF polyclonal antibody (*A*, *C*, *E*, and *G*) or anti-LCCL monoclonal antibody (*B*, *D*, *F*, and *H*). The *arrowheads* point to the 120-kDa mutant-specific band (dimer cochlin (*DI-Coch*)), full-length cochlin (*FL-Coch*), CTF, and NTF.

cochlin is similar under reducing and nonreducing conditions. Interestingly, in all samples of the culture supernatant and cell lysates collected from the cells expressing cochlin mutants, an additional 120-kDa band recognized by both anti-CTF and anti-LCCL antibodies on Western blots was observed (Fig. 3, *A*, *B*, *E*, and *F*, *arrowheads*). The migratory behavior of full-length cochlin upon nonreducing SDS-PAGE suggests that the 120-kDa band constitutes a dimer of cochlin. This result suggests that all DFNA9-associated cochlin mutants misfold and form dimers, although the efficiency of dimerization may be different: P53S and G90E cochlins appear to form dimers much more readily compared with V68G and W119R cochlins. The migratory behavior of misfolded cochlin mutants is similar, as they all migrated as a 120-kDa band in the presence of SDS without reducing agent.

To further characterize this 120-kDa band, we treated the culture supernatant and cell lysates collected from cells expressing WT and mutant cochlins with the reducing agent β-mercaptoethanol and analyzed the results by reducing SDS-PAGE and Western blotting. As shown in Fig. 3 (*C*, *D*, *G*, and *H*), the addition of β-mercaptoethanol completely eliminated the presence of this 120-kDa band in the culture supernatant and cell lysates from cells expressing the mutant cochlin. On the basis of these results, we conclude that the mutant-specific 120-kDa band detected by both anti-CTF and anti-LCCL antibody is highly sensitive to reducing conditions. Considering that β-mercaptoethanol reduces disulfide bonds in proteins, this result suggests that the mutations in cochlin may result in the formation of abnormal disulfide bonds. On the other hand, because a significant amount of misfolded mutant cochlin is detected in the culture supernatant and cell lysates, it appears that protein misfolding *per se* is not sufficient to result in their

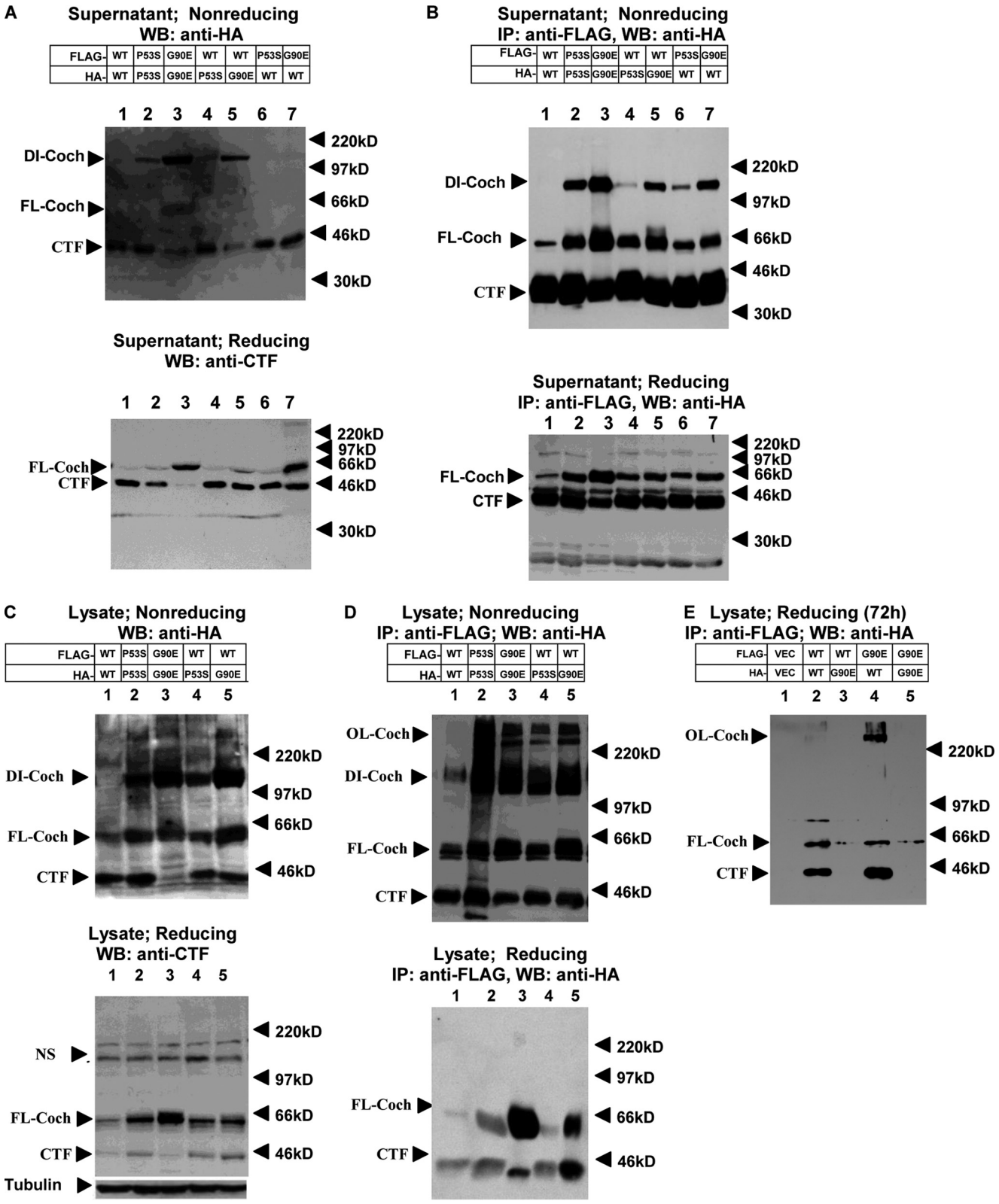

FIGURE 4. **Dimerization of cochlins.** HEK293T cells were cotransfected with HA- or FLAG-tagged WT, P53S, or G90E cochlin as indicated at a 1:1 ratio. Forty-eight hours after transfection (*A–D*), supernatants and lysates were collected. Western blotting (*WB*) of the culture supernatant (*A* and *B*) and cell lysates (*C* and *D*) was performed using anti-HA antibody after separation by 8% nonreducing SDS-PAGE (*A* and *C*, *upper panels*) or anti-CTF antibody after separation by 12% reducing SDS-PAGE (*A* and *C*, *lower panels*). The collected culture supernatant and lysates (*B* and *D*) were used to perform immunoprecipitation (*IP*) with anti-FLAG antibody-conjugated agarose beads. After washing, the FLAG immunocomplexes were eluted with FLAG peptide, and the eluates were analyzed by 8% nonreducing SDS-PAGE (*B* and *D*, *upper panels*) or 12% reducing SDS-PAGE (*B* and *D*, *lower panels*). The Western blots were probed with anti-HA antibody. The bands at ~220 kDa in *C* (both *upper* and *lower panels*) are nonspecific. *NS*, nonspecific band. Cell lysates were collected 72 h after transfection, and 12% SDS-PAGE was conducted under reducing conditions (*E*). The Western blots were probed with anti-HA antibody. The results shown are representative of three independent experiments. *DI-Coch*, dimer cochlin; *FL-Coch*, full-length cochlin; *OL-Coch*, oligomer cochlin.

retention in the endoplasmic reticulum and/or selective degradation through ER-associated protein degradation (26).

Dimeric Interactions of WT and Mutant Cochlins—To gain further insight into the cellular events that lead to cochlin misfolding and dimerization, we constructed HA- and FLAG-tagged WT, P53S, and G90E cochlin expression vectors and transiently transfected them pairwise into HEK293T cells. In culture supernatant from cells expressing WT cochlin, anti-HA Western blotting detected predominantly CTF (44 kDa) (Fig. 4*A*, *upper panel*), consistent with the efficient processing of WT cochlin after its secretion. Immunoprecipitation using anti-FLAG antibody from cells expressing two expression vectors of FLAG-tagged WT cochlins pulled down a significant amount of HA-tagged CTF as well as a small amount of full-length cochlin (Fig. 4*B*, *upper panel*). Although the dimers were disrupted by the presence of reducing agent, the interaction of secreted full-length and CTF cochlins could still be detected (Fig. 4*B*, *lower panel*), including WT cochlin. Thus, cochlin may normally dimerize, and the dimerization of mutant cochlin may be further stabilized by disulfide bonds.

In the supernatant of cell cultures expressing mutant cochlin alone or WT and mutant cochlins together, different amount of the dimer (120 kDa), full-length cochlin, and CTF could be detected by Western blotting (Fig. 4*A*). Anti-FLAG antibody from the supernatant of cells expressing both FLAG- and HA-tagged mutant cochlins could immunoprecipitate HA-tagged mutant cochlin (Fig. 4*B*, *upper panel*), confirming that the 120-kDa species is indeed a dimer. Interestingly, WT cochlin, which could not be detected as a 120-kDa dimer in the supernatant after nonreducing SDS-PAGE when expressed alone, was found to interact with mutant cochlin as part of a 120-kDa dimer when coexpressed with mutant cochlin (Fig. 4*B*, *upper panel*). Thus, the interaction between WT and mutant cochlins leads to the formation of misfolded dimers that persist after secretion, similar to that with mutant cochlin alone, suggesting that WT cochlin can be recruited to and form stable dimers with mutant cochlin.

We next investigated whether the dimers could be detected intracellularly. The interaction of intracellular WT and mutant cochlins was also detected using immunoprecipitation in cells expressing two differentially tagged cochlin-expressing vectors (Fig. 4, *C* and *D*). Interacting mutant and WT cochlins were found to be present as 120-kDa dimers as well as in higher molecular mass oligomers after nonreducing SDS-PAGE. Interestingly, when WT cochlin was expressed alone, a small amount of WT cochlin was also present as a 120-kDa dimer in cell lysates, suggesting that WT cochlin might form disulfide bond-stabilized dimers intracellularly in a transient manner, with reduced affinity and/or with reduced rate of dimer formation, whereas interacting mutant and WT cochlins persist in dimer conformation even after secretion.

In the supernatant and lysates collected from cells expressing WT and mutant cochlins for 48 h and analyzed under reducing conditions, all dimers and oligomers were efficiently disrupted (Fig. 4, *A–D*, *lower panels*), suggesting that misfolded cochlin is initially sensitive to reducing conditions. Interestingly, in lysates collected from cells expressing WT or mutant cochlin for 72 h, a higher molecular mass complex of WT cochlin resistant to reducing agents (>220 kDa) was immunoprecipitated using anti-FLAG antibody for mutant cochlin (Fig. 4*E*), suggesting that WT cochlin may be induced to form highly stable oligomers in the presence of mutant cochlin.

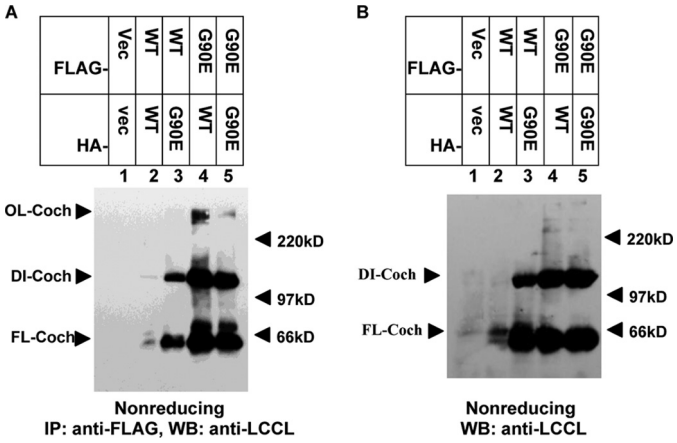

FIGURE 5. **WT and mutant cochlin oligomerization in UB/UE-1 cells.** UB/UE-1 cells were cotransfected with HA- and FLAG-tagged WT and mutant G90E cochlins as indicated at a 1:1 ratio. Cochlin was detected by immunoprecipitation (*IP*) using anti-FLAG antibody, and the Western blot (*WB*) was probed with anti-LCCL antibody after 8% nonreducing SDS-PAGE (*A*). Also shown is a control Western blot probed with anti-LCCL antibody after nonreducing SDS-PAGE of the cell lysates shown in *A* (*B*). *Vec*, vector; *DI-Coch*, dimer cochlin; *OL-Coch*, oligomer cochlin; *FL-Coch*, full-length cochlin.

Next, we investigated whether the misfolding event of mutant cochlin observed in 293T cells is relevant to DFNA9 hearing loss using UB/UE-1 cells derived from the inner ear. On the Western blots of cell lysates analyzed by nonreducing SDS-PAGE, anti-LCCL antibody detected the same mutant 120-kDa dimer as well as higher molecular mass oligomers in cells expressing mutant cochlin or WT and mutant cochlins together but not WT cochlin alone (Fig. 5). These results suggest that the formation of mutant cochlin and the WT and mutant cochlin complex occurs similarly in differentiated UB/UE-1 cells as in 293T cells, providing a validation for our analysis in 293T cells.

Hearing Impairment Induced by Mutant Cochlin in Vivo—Because mutant cochlins are processed differently from WT cochlin (Figs. 3 and 4) and because mutant cochlin recruits WT cochlin to form oligomeric complexes, we asked whether inoculation with mutant cochlin could impair hearing ability in wild-type mice *in vivo*. We collected CM from 293T cells expressing WT or G90E (corresponding to human DFNA9 mutation G88E) cochlin and injected CM directly into the cochleae of mice. One and 4 weeks after injection, hearing thresholds were examined by ABR testing. As shown in Fig. 6, mice injected with CM containing WT cochlin showed no significant changes in ABR thresholds either 1 or 4 weeks after injection, whereas mice injected with mutant cochlin showed an increase of ~40 db in ABR thresholds. The functional changes induced by mutant cochlin were dramatic: most of the mice were nearly deaf 1 week after injection, although some of them recovered slightly 4 weeks after injection (Fig. 6*A*). This observation strongly suggests that the administration of mutant cochlin leads to chronic hearing impairment.

To determine at the cellular level how the mutant cochlin causes hearing loss, we conducted histological analysis to

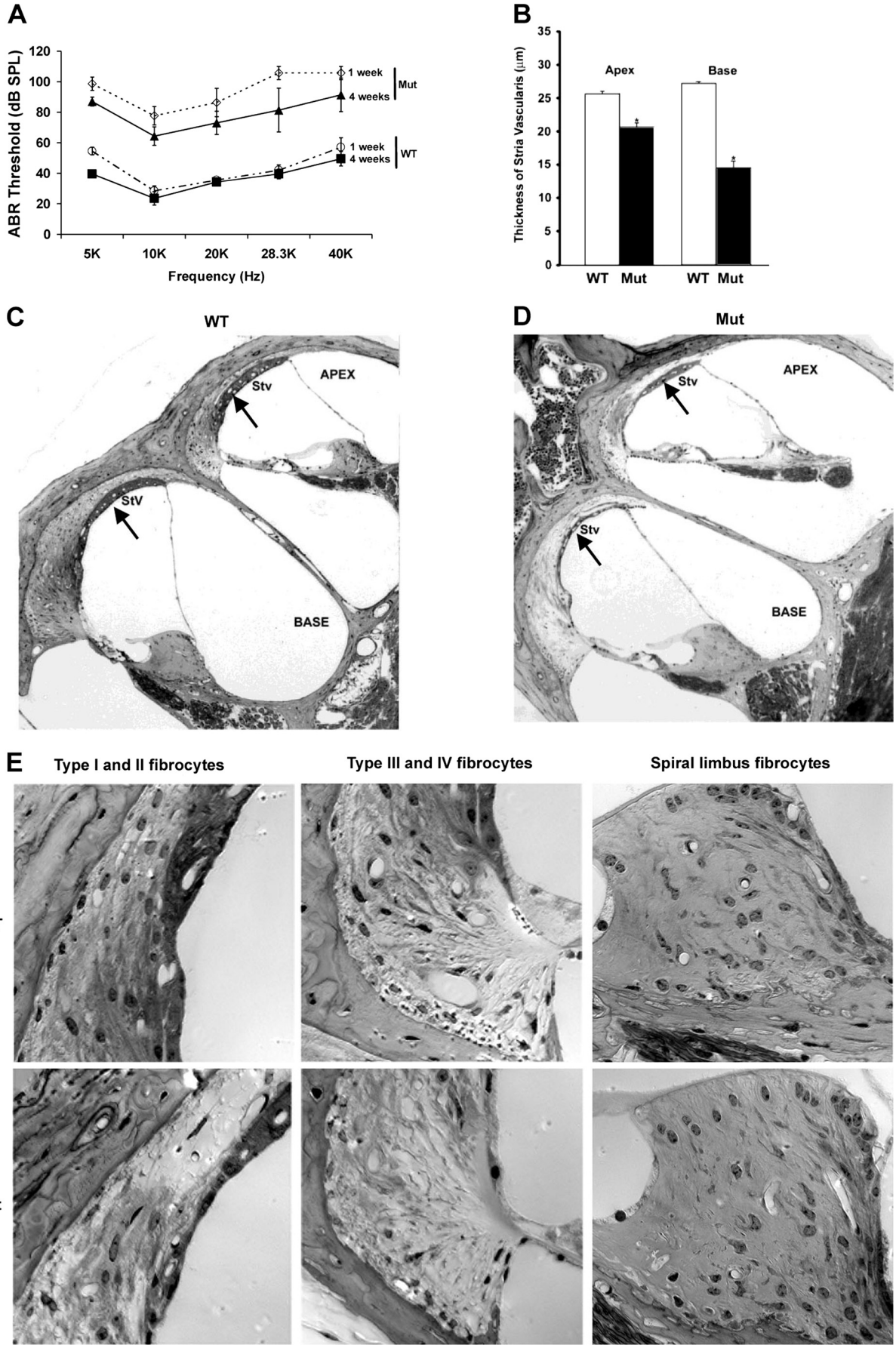
A
ABR Threshold (dB SPL)
120
100
80
60
40
20
0
1 week
4 weeks
Mut
1 week
4 weeks
WT
5K
10K
20K
28.3K
40K
Frequency (Hz)
B
Thickness of Stria Vascularis (μm)
35
30
25
20
15
10
5
0
Apex
Base
WT
Mut
WT
Mut
C
WT
APEX
Stv
StV
BASE
D
Mut
APEX
Stv
Stv
BASE
E
Type I and II fibrocytes
Type III and IV fibrocytes
Spiral limbus fibrocytes
WT
Mut

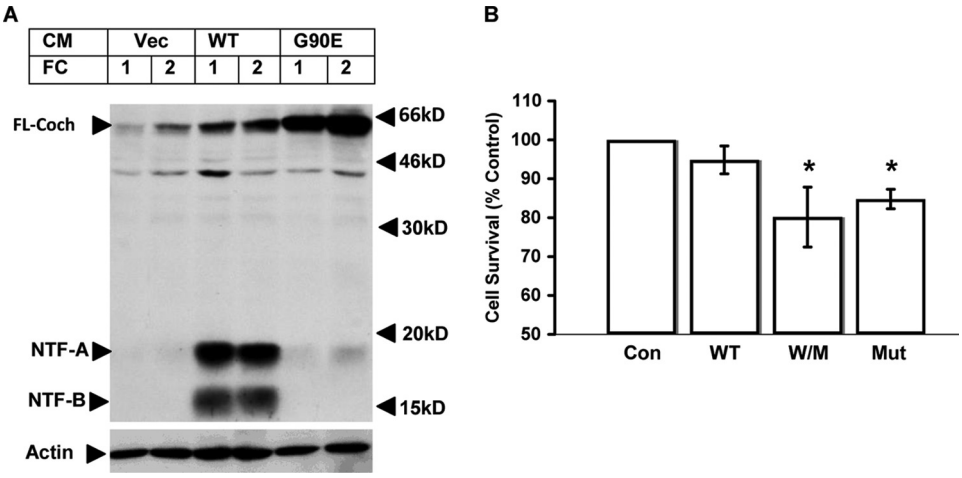

FIGURE 7. **Extracellular mutant cochlin binds to primary fibrocytes and reduces cell survival.** *A*, fibrocytes (*FC*) from WT mice were isolated and cultured *in vitro* and treated with CM (1:5 dilution) collected from transiently transfected HEK293T cells expressing vehicle control (*Vec*) or WT or mutant G90E cochlin. After treatment, the supernatant was removed, and cells were washed twice with phosphate-buffered saline. The cell lysates were analyzed by 15% reducing SDS-PAGE, followed by Western blotting using anti-LCCL antibody. *B*, primary fibrocytes were incubated with CM from 293T cells expressing vehicle (*Con*), WT cochlin alone, WT and mutant G90E cochlins together (*W/M*), or mutant G90E cochlin alone (*Mut*) for 72 h. Cell survival was measured using the MTS assay. *, $p < 0.05$. *FL-Coch*, full-length cochlin.

examine whether injection of CM containing mutant cochlin would disrupt the cochlear structure. We observed changes in the thickness of the stria vascularis in mice injected with CM containing mutant cochlin compared with mice injected with CM containing WT cochlin and further quantified this difference in both the apex and base canal of the cochlea (Fig. 6, *B–D*). Interestingly, an extensive loss of fibrocytes I–IV in the spiral ligament was easily observed after one injection of mutant cochlin, whereas fibrocytes in the spiral limbus were largely spared (Fig. 6*E*). These results suggest that stria vascularis cells and fibrocytes of the spiral ligament are highly sensitive to the insult of injected misfolded extracellular mutant cochlins, consistent with a prominent loss of fibrocytes as found in pathological specimens of DFNA9 (3).

Extracellular Mutant Cochlin Exhibits Cytotoxicity to Primary Fibrocytes—Because our *in vivo* injection experiments suggested that mutant cochlin might exhibit an extracellular cytotoxicity to fibrocytes of the inner ear, we set out to test this possibility directly *in vitro*. We first asked whether the extracellular cochlin can be retained by primary fibrocytes derived from the cochlea. As shown in Fig. 7*A*, after incubating primary fibrocytes with CM from 293T cells expressing WT or mutant cochlin, significant amounts of both WT and mutant cochlins were detected in the cell lysates of primary fibrocytes. Thus, extracellular cochlin adhered to and/or was taken up by primary fibrocytes.

To determine whether the extracellular mutant cochlin may be cytotoxic to primary fibrocytes, we incubated primary fibrocytes with CM from 293T cells expressing WT and mutant cochlins for 72 h and measured cell survival. Although incubation of WT CM did not affect the survival of primary fibrocytes, incubation of WT/mutant CM or mutant CM alone significantly decreased cell survival (Fig. 7*B*). These results suggest that the extracellular mutant cochlin can be retained by primary fibrocytes and is cytotoxic to primary fibrocytes *in vitro*, consistent with the ability of injected mutant cochlin to induce fibrocyte death in the cochlea, leading to damage in the cochlear structure and loss of hearing ability of mice *in vivo* (Fig. 6).

DISCUSSION

In this study, we examined the processing and secretion of full-length WT and mutant cochlins in fibrocytes of the inner ear using two anti-cochlin antibodies developed in our laboratory. We found that the generation of the 18- and 16-kDa LCCL domain isoforms is differentially affected by the DFNA9-associated cochlin mutations. On the basis of a biochemical assay using nonreducing SDS-PAGE and Western blotting, we further found that the expression of DFNA9-associated cochlin mutants leads to early dimerization and oligomerization and the eventual formation of reducing agent-insensitive oligomers. Importantly, we have discovered the ability of mutant cochlin to interact with and to mediate dimerization and oligomerization with WT cochlin and the formation of reducing agent-resistant WT oligomers. On the basis of these *in vitro* biochemical data, we hypothesize that mutant cochlin oligomers may contribute to hearing loss by inducing the degeneration of the stria vascularis and the death of fibrocytes in the spiral ligament *in vivo*. Our study suggests that protein misfolding might provide an important mechanism underlying the DFNA9 pathology.

The structural features of the LCCL domain might play an important role in the dimerization and oligomerization of WT and mutant cochlins. The LCCL domain represents an unusual fold with a centrally located α-helix wrapped by two β-sheets and a highly irregular secondary structure with an extended polypeptide (7). Disulfide bonds in the WT LCCL domain are predicted to form between Cys^{8} and Cys^{24} and between Cys^{28} and Cys^{48}, although alternative possibilities have not been ruled out. Because most DFNA9-associated *COCH* mutations involve residues on the cochlin surface and because all four cysteine sulfurs are close in space, it is conceivable that these mutations lead to mispairing of cysteines during oxidative for-

FIGURE 6. **Mutant cochlin induces hearing loss and histological changes in the cochlea.** WT and mutant G90E (*Mut*) cochlins were transiently expressed in HEK293T cells. Special culture medium without fetal bovine serum and antibiotics (CM) was collected and concentrated and then injected into the cochleae of adult C57BL/6 mice ($n = 4$), and the ABR thresholds were measured 1 and 4 weeks after injection (*A*). The thickness of the stria vascularis (*Stv*) was measured in hematoxylin/eosin-stained mouse inner ears (*B*). The morphological changes in mouse cochleae injected with WT CM (*C*) and mutant G90E cochlin (*D*) collected at 4 weeks after injection are shown (*, $p < 0.05$, *t* test), with *arrows* pointing to the stria vascularis. Four different types of fibrocytes affected by injection of G90E CM are clearly observed in the spiral ligament (*SPL*) but not in the spiral limbus (*E*).

mation of the disulfide bridges. The extended β-sheets on the surface of the LCCL domain may also be important in mediating misfolding. Although the expression of mutant cochlin alone is sufficient to lead to dimerization and oligomerization of itself as well as to the stabilization of WT cochlin in the dimer and oligomer conformation, the presence of WT cochlin in the complex may further stabilize the oligomer conformation. Structural analysis of a seven-residue peptide from yeast prion Sup35 showed a double β-sheet, which may play a key role in the formation of stable amyloid fibrils (27). This has led to the "exposed β-sheet hypothesis," in which the transition to the β-sheet dominant conformation plays a key role in mediating neurotoxicity (28). Future studies are needed to test whether DFNA9-associated cochlin mutations are another example of such exposed β-sheet-mediated protein misfolding.

The nature of DFNA9 mutant cochlin-mediated misfolding shows a critical difference compared with mutant Htt, which, upon expression in mammalian cells, rapidly forms highly insoluble microscopic visible aggregates that are irregular in shape and size. On the other hand, misfolded mutant cochlin does not seem to form microscopically visible aggregates at least 3 days after expression in mammalian cells. However, because coexpression of WT and mutant cochlins does eventually lead to the formation of reducing agent-resistant oligomers detectable by Western blotting after transfection for 72 h, the characteristic eosinophilic and microfibrillar deposits in DFNA9-affected inner ears (29) could represent the accumulation of such misfolded WT and mutant cochlins. Future experiments are needed to test this hypothesis directly. The slow kinetic behavior of DFNA9-associated mutant and WT cochlins in dimerization and oligomerization presents an interesting opportunity for us to examine the cellular and biochemical mechanisms by which mutant and WT protein interactions lead to protein misfolding.

We have shown that the expression of mutant and WT cochlins in UB/UE-1 cells induces cell death. Furthermore, we have shown that extracellular cochlin interacts with primary fibrocytes and that the presence of extracellular mutant cochlin induces cytotoxicity in primary cultured fibrocytes. Because extracellular cochlin provided as CM from 293T cells expressing WT or mutant cochlin exhibits certain selectivity, as the binding to primary fibrocytes is more efficient than that of HeLa cells (data not shown), fibrocytes might express a receptor for cochlin. Interestingly, mutant cochlin delivered directly into the cochlea *in vivo* appears to exhibit some selective cytotoxicity toward the stria vascularis and fibrocytes in the spiral ligament. However, the fibrocytes in the spiral limbus are largely unaffected. Because a selective loss of fibrocytes is one of the characteristic pathological features of DFNA9 (3), we suggest that we have established both culture and animal models that can be used for further studies of the mechanism involved in DFNA9.

We propose that misfolding of mutant and WT cochlins in dimers and oligomers leads to a toxic gain of function that is responsible for the cellular degeneration and hearing loss in DFNA9 patients. Recently, an interesting *Coch* G88E knock-in mutant mouse was made (8). Vestibular function was affected in $Coch^{G88E/G88E}$ homozygous mutant mice starting from 11 months of age, when cochlear function was still normal. Defective cochlear function was detected only at advanced ages in both $Coch^{G88E/G88E}$ homozygous and $Coch^{G88E/+}$ heterozygous mutant mice. No loss of cellularity or eosinophilic deposits characteristic of DFNA9 was observed in $Coch^{G88E/G88E}$ homozygous mutant mice. Because DFNA9 syndrome in humans leads to late-onset hearing loss, aging might play an important role in triggering the onset of hearing loss in DFNA9 syndrome. This situation may be similar to many other late-onset neurodegenerative diseases such as Huntington disease, where patients may live unsymptomatic for decades before the onset of disease. Furthermore, cell death is rarely observed in mouse models of Huntington disease, whereas selective neurodegeneration is a key feature of end-stage polyglutamine diseases such as Huntington disease (30). On the other hand, mutant Htt with expanded polyglutamine forms aggregates *in vitro* and in cell culture models and induces cell death (31). We propose that aging may negatively impact on the ability to clear both intracellular and extracellular misfolded cochlin in the inner ears of DFNA9 patients and lead to the eventual onset of deafness. Because none of the experimental models can completely mimic the *in vivo* condition, a combination of different model systems is needed for us to explore the mechanism that leads to the onset of age-dependent neurodegeneration such as DFNA9.

Acknowledgments—We thank Caroline Yi and Andrew Steele for critical reading of the manuscript.

REFERENCES

1. Bossy-Wetzel, E., Schwarzenbacher, R., and Lipton, S. A. (2004) *Nat. Med.* **10,** (suppl.) S2–S9
2. Robertson, N. G., Lu, L., Heller, S., Merchant, S. N., Eavey, R. D., McKenna, M., Nadol, J. B., Jr., Miyamoto, R. T., Linthicum, F. H., Jr., Lubianca Neto, J. F., Hudspeth, A. J., Seidman, C. E., Morton, C. C., and Seidman, J. G. (1998) *Nat. Genet.* **20,** 299–303
3. Merchant, S. N., Linthicum, F. H., and Nadol, J. B., Jr. (2000) *Adv. Otorhinolaryngol.* **56,** 212–217
4. Khetarpal, U., Schuknecht, H. F., Gacek, R. R., and Holmes, L. B. (1991) *Arch. Otolaryngol. Head Neck Surg.* **117,** 1032–1042
5. Robertson, N. G., Skvorak, A. B., Yin, Y., Weremowicz, S., Johnson, K. R., Kovatch, K. A., Battey, J. F., Bieber, F. R., and Morton, C. C. (1997) *Genomics* **46,** 345–354
6. Nagy, I., Trexler, M., and Patthy, L. (2008) *FEBS Lett.* **582,** 4003–4007
7. Liepinsh, E., Trexler, M., Kaikkonen, A., Weigelt, J., Bányai, L., Patthy, L., and Otting, G. (2001) *EMBO J.* **20,** 5347–5353
8. Robertson, N. G., Jones, S. M., Sivakumaran, T. A., Giersch, A. B., Jurado, S. A., Call, L. M., Miller, C. E., Maison, S. F., Liberman, M. C., and Morton, C. C. (2008) *Hum. Mol. Genet.* **17,** 3426–3434
9. Makishima, T., Rodriguez, C. I., Robertson, N. G., Morton, C. C., Stewart, C. L., and Griffith, A. J. (2005) *Hum. Genet.* **118,** 29–34
10. Rodriguez, C. I., Cheng, J. G., Liu, L., and Stewart, C. L. (2004) *Endocrinology* **145,** 1410–1418
11. Ikezono, T., Omori, A., Ichinose, S., Pawankar, R., Watanabe, A., and Yagi, T. (2001) *Biochim. Biophys. Acta* **1535,** 258–265
12. Ikezono, T., Shindo, S., Li, L., Omori, A., Ichinose, S., Watanabe, A., Kobayashi, T., Pawankar, R., and Yagi, T. (2004) *Biochem. Biophys. Res. Commun.* **314,** 440–446
13. Robertson, N. G., Resendes, B. L., Lin, J. S., Lee, C., Aster, J. C., Adams, J. C., and Morton, C. C. (2001) *Hum. Mol. Genet.* **10,** 2493–2500

14. Grabski, R., Szul, T., Sasaki, T., Timpl, R., Mayne, R., Hicks, B., and Sztul, E. (2003) *Hum. Genet.* **113,** 406–416
15. Robertson, N. G., Hamaker, S. A., Patriub, V., Aster, J. C., and Morton, C. C. (2003) *J. Med. Genet.* **40,** 479–486
16. Scherzinger, E., Lurz, R., Turmaine, M., Mangiarini, L., Hollenbach, B., Hasenbank, R., Bates, G. P., Davies, S. W., Lehrach, H., and Wanker, E. E. (1997) *Cell* **90,** 549–558
17. Glenner, G. G., and Wong, C. W. (1984) *Biochem. Biophys. Res. Commun.* **122,** 1131–1135
18. Li, H., Zhu, H., Xu, C. J., and Yuan, J. (1998) *Cell* **94,** 491–501
19. Lawlor, P., Marcotti, W., Rivolta, M. N., Kros, C. J., and Holley, M. C. (1999) *J. Neurosci.* **19,** 9445–9458
20. Suko, T., Ichimiya, I., Yoshida, K., Suzuki, M., and Mogi, G. (2000) *Hear. Res.* **140,** 137–144
21. Nakagawa, T., Kim, T. S., Murai, N., Endo, T., Iguchi, F., Tateya, I., Yamamoto, N., Naito, Y., and Ito, J. (2003) *Hear. Res.* **176,** 122–127
22. Iguchi, F., Nakagawa, T., Tateya, I., Endo, T., Kim, T. S., Dong, Y., Kita, T., Kojima, K., Naito, Y., Omori, K., and Ito, J. (2004) *Acta Otolaryngol. Suppl.* 43–47
23. Shen, H., Zhang, B., Shin, J. H., Lei, D., Du, Y., Gao, X., Wang, Q., Ohlemiller, K. K., Piccirillo, J., and Bao, J. (2007) *Hear. Res.* **226,** 52–60
24. Ohlemiller, K. K., McFadden, S. L., Ding, D. L., Lear, P. M., and Ho, Y. S. (2000) *J. Assoc. Res. Otolaryngol.* **1,** 243–254
25. Whittaker, C. A., and Hynes, R. O. (2002) *Mol. Biol. Cell* **13,** 3369–3387
26. Rose, J. K., and Doms, R. W. (1988) *Annu. Rev. Cell Biol.* **4,** 257–288
27. Nelson, R., Sawaya, M. R., Balbirnie, M., Madsen, A. Ø., Riekel, C., Grothe, R., and Eisenberg, D. (2005) *Nature* **435,** 773–778
28. Nagai, Y., and Popiel, H. A. (2008) *Curr. Pharm. Des.* **14,** 3267–3279
29. Khetarpal, U. (2000) *Laryngoscope* **110,** 1379–1384
30. Ferrante, R. J. (2009) *Biochim. Biophys. Acta* **1792,** 506–520
31. Lipinski, M. M., and Yuan, J. (2004) *Curr. Opin. Pharmacol.* **4,** 85–90